HiSST: 2nd International Conference on High-Speed Vehicle Science & Technology

11–15 September 2022, Bruges, Belgium

Transpiration Cooling under Supersonic Rocket Engine Nozzle Flow Conditions

Jonas Peichl[1], Markus Selzer[1], Hannah Böhrk[1,2], Andreas Schwab[3], Bastian Hammer[4], Sandra Ludescher[4,5], Karl Alexander Heufer[4]

Abstract

In a preliminary feasibility study, transpiration cooling in the supersonic flow of a conical laval type nozzle is investigated. Hot gas flow with the flow conditions of a rocket engine nozzle is created via a detonation tube combusting hydrogen and oxygen at a stagnation pressure of 30 bar with a hot gas flow Mach number of Ma = 3.35 at the beginning of the coolant injection. In this context, a variation of the transpired coolant mass flow rate, using helium as a coolant gas, was conducted. Special emphasis is laid on the heat flux reduction on both the transpiration cooled segment as well as the solid nozzle structure in the wake flow. As result, cooling efficiencies of up to 0.85 at the end of the porous sample could be measured. For the creation of an cooling film, it could be shown that comparably high blowing ratios are needed for creating a lasting cooling film.

Keywords: *transpiration cooling, expansion nozzle cooling, detonation tube*

Nomenclature

Latin

A – area
c_p – specific heat capacity at constant pressure
D – diameter
F – blowing ratio
h – heat transfer coefficient
k – thermal conductivity
M – Mach number
p – pressure
$\dot{m}$ – mass flow
$\dot{q}$ – heat flux
r – radius
Re – Reynolds number
s – slot height
T – temperature
t – time
u – velocity

Greek

δ – boundary layer thickness
ρ – density
γ – isentropic coefficient
μ – dynamic viscosity
η – cooling efficiency
ϕ – angular specific mass flow rate

Subscripts

0 – state at stagnation point
c – coolant, cooled
curv – curvature
CR – coolant reservoir
Film – film cooling
hg – hot gas
nc – without cooling
TI – specimen plenum
Transpiration – transpiration cooling
vn – Venturi
w – state at wall

[1] *Institute for Structures and Design, German Aerospace Center (DLR), Pfaffenwaldring 38-40, 70569 Stuttgart, Germany, Jonas.Peichl@dlr.de*

[2] *Now at DHBW Stuttgart*

[3] *Institute for Aerospace Thermodynamics, University of Stuttgart, Pfaffenwaldring 31, 70659 Stuttgart Germany*

[4] *Chair of High Pressure Gas Dynamics, Shock Wave Laboratory, RWTH Aachen University, Schurzelter Str. 35, 52074 Aachen, Germany*

[5] *Now at Hyimpulse Technologies GmbH*

1. Introduction

High demands are placed on the nozzle structure of chemical propulsion systems for future space transportation systems. Increasing thermal and mechanical loads and the demand for increased structural life time for reusable launch vehicles are driving factors for the current development. Therefore, an effective cooling system is required to reduce the incoming heat flux while also meeting mass and cost constraints. The nozzle extensions of main stage rocket engines are nowadays actively cooled, employing multiple cooling methods like regenerative or dump cooling [1]. For extreme thermal load cases, additional film cooling is being applied by injecting the gas generator turbine exhaust gas tangential to the nozzle wall and forming a protective coolant layer between the hot gas main flow and the nozzle wall. The latter coolant system is applied for example in the Vulcain 2 or F-1 rocket engines [2].

Due to the expected further increase of combustion chamber pressures and subsequently increasing thermal loads on the nozzle structure, transpiration cooling is being considered as a viable option for coping with these loads. This cooling method is characterized by a high effectiveness and efficiency compared to other cooling methods, which is shown e.g. in Eckert and Livingood [3]. Here, the coolant fluid is forced through a permeable wall and injected orthogonally to the hot gas flow. The high cooling efficiency is caused by two distinctive mechanisms. On the one hand, while flowing through the porous structure, the coolant fluid exchanges heat within the porous material. On the other hand, the transpiring coolant forms a protective layer above the wall, effectively reducing the incoming heat flux on the wall. The principles of transpiration and film cooling are illustrated in Fig. 1.

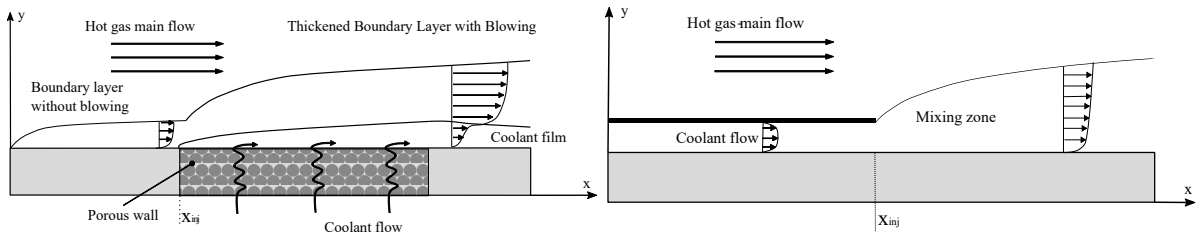

(a) Transpiration cooling [4] (b) Film cooling [5]

Fig 1. Schematic description of transpiration and film cooling

While transpiration cooling is well investigated for flat plates under subsonic and supersonic flow conditions for example by Langener et. al. [4], only few experimental data of transpiration cooling under supersonic nozzle flow conditions exist. Early studies on transpiration cooling in supersonic nozzle flow focused mainly on the heat transfer reduction through the cooling film in the wake flow of a porous segment. The porous segment was either placed in the convergent, subsonic part of the nozzle as described in Librizzi and Cresci [6] or in the divergent, supersonic part as in Goldstein et al. [7]. The effect on the heat transfer on a porous nozzle throat and divergent section under supersonic flow conditions in a shock tube facility was investigated by Chen et al. [8] and Keener et al. [9] utilizing an air-helium mixture as hot gas and air as the coolant fluid. A significant reduction of the heat flux by 14 % at a local blowing ratio of 0.51% [9] and of 40% at a blowing ratio of 1.17% [8] compared to the heat flux without cooling could be measured. Only a minimal impact on the specific impulse and thrust coefficient was determined.

The objective of this preliminary study is to compare the heat transfer characteristics of film and transpiration cooling under supersonic nozzle flow conditions. Extensive studies of supersonic film cooling in a generic conical nozzle were performed at the Shock Wave Laboratory (SWL) of the RWTH Aachen by Ludescher [10, 11]. The experimental setup is a detonation-tube facility. By combusting a hydrogen/oxygen mixture, a hot gas flow with stagnation pressures up to 150 bar and stagnation temperatures of 3800 K can be achieved.
For investigating transpiration cooling under supersonic conditions, this facility is equipped with a porous specimen in the divergent nozzle section, beginning with the coolant injection at a hot gas Mach number

of M = 3.35. Both the heat flux reduction on the surface of the porous sample and the influence on the nozzle wall heat flux in the wake flow of a transpiration cooled segment are investigated.

2. Experimental Approach and Setup

In the following section, a description of the detonation tube facility is given. Furthermore, the permeable transpiration cooling specimen is described in detail as well as the determination process for the experimental parameters.

2.1. Shock Tube Facility

The transpiration cooling experiments were performed in a short-duration facility for simulating rocket engine nozzle flow conditions, which is based on the detonation-tube technique. The facility was designed by Yahiaoui and Olivier [12]. It consists of four sections as shown in Fig. 2: a damping section of 3 m length, a detonation tube of 10 m length with an attached axisymmetric nozzle and a vacuum tank. The sections are separated with diaphragms before flow initiation. Whereas a 1 mm-thick steel diaphragm is used to separate the nozzle stagnation chamber from the detonation tube, a 0.2-mm-thick PE diaphragm is placed between the detonation tube and the damping section.

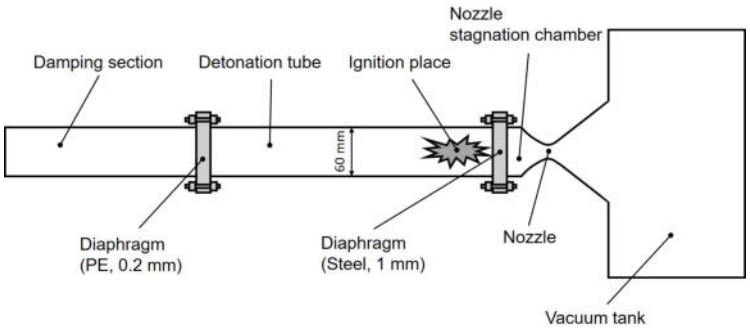

Fig 2. Scheme of test facility

The detonation tube provides the high enthalpy flow which is needed for the stagnation conditions of the rocket-engine-like flow. The vacuum tank delivers a low pressure outlet at the nozzle exit and thus guarantees a supersonic nozzle flow during the measurement time. Also the damping section, which is connected to one end of the detonation tube, is evacuated with a rotary vane pump to a pressure below 0.1 mbar before detonation. Therefore, it reduces the thermal and mechanical loads of the incoming detonation wave at the end wall as well as prolongs the testing time. The flow medium is a premixed hydrogen-oxygen gas which is ignited with a 1.3 kV electric spark. After ignition, a detonation wave forms which reaches the diaphragm next to the nozzle first and leads to an almost instantaneous diaphragm burst due to the pressure rise across the detonation wave. The Taylor expansion behind the detonation wave slows down the burnt gas to very low velocities in the nozzle plenum chamber [10]. The usable testing time for transpiration and film cooling experiments is between 2-5 ms. The stagnation conditions can be varied by changing the initial conditions of the combustion [10]. The hot gas conditions for the present investigation are listed in Table 1.

Table 1. Hot gas parameters

Condition	Symbol	Unit	Value
Stagnation temperature	T_0	K	3660
Stagnation pressure	p_0	bar	30
Oxidizer/fuel mixture ratio	ROF	-	8
Wall temperature	T_w	K	330

In order to prevent condensation of the hot gaseous water at the inner walls of the facility, an electrical heating system with a heating power of about 100 W/m^2 has been installed. This heating system allows wall temperatures up to 373 K. Thermocouples of type K are mounted directly on the outer tube and the nozzle surface. A separated temperature controller ensures the control and regulation of the heating system. A rock wool insulation of 50 mm thickness reduces heat losses and leads to a uniform wall temperature distribution [10].

For investigating supersonic film cooling for rocket engine nozzles, a conical laval-type nozzle was installed. For the present campaign, the nozzle has been equipped with a transpiration coolant specimen, which is placed downstream of the nozzle throat as shown in Fig. 3.

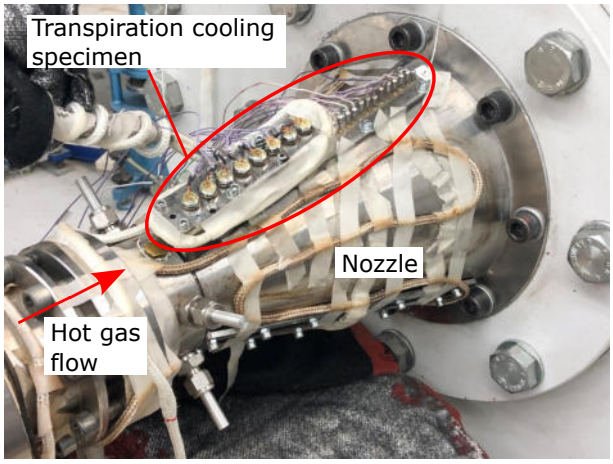

Fig 3. Photography of investigated nozzle equipped with transpiration cooling specimen

2.2. Transpiration Cooling Specimen

The specimen for the transpiration cooling experiments is depicted in Fig. 4. In order to allow an easy implementation into the existing facility, only a small transpiration cooling insert has been considered in this preliminary feasibility study, knowing that this probably leads to considerable three-dimensional flow effects as discussed later. The porous section of the specimen consists of a 110 x 8 mm^2 sized slice of porous carbon fiber reinforced carbon (C/C) with a thickness of 7 mm. The hot gas side specimen face is contoured concavely to match the nozzle geometry. To prevent lateral flow and to create a

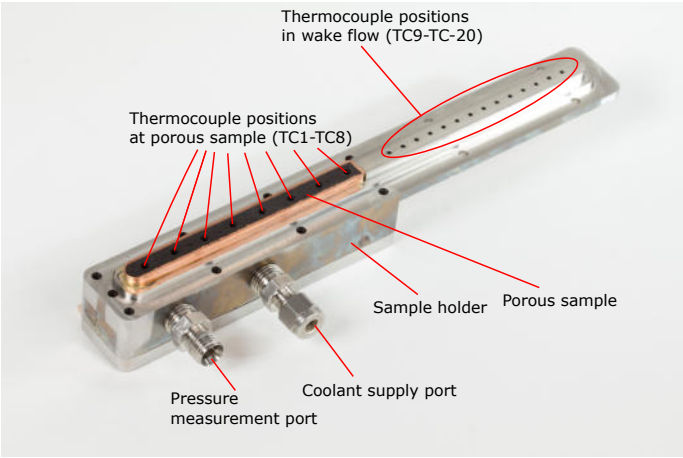

Fig 4. Depiction of the transpiration cooling specimen

defined outflow surface the specimen side faces were sealed with electroplated copper. The framed

porous sample is adhered into a stainless steel sample holder, which also acts as a plenum chamber for the coolant gas. To assess the heat flux on the nozzle structure, the specimen is equipped with a total of 20 type-E coaxial thermocouples with a diameter of 1.9 mm. Eight thermocouples (TC 1-TC 8) are placed on the surface of the porous sample. Another twelve thermocouples (TC9-TC20) are placed on the nozzle wall surface downstream to the porous sample for assessing the effect of the transpired wake flow on the wall heat flux. The thermocouple measurements were conducted with a sampling rate of 250 kHz. Using the method developed by Cook [13], the heat flux on the nozzle wall is determined by

$$\dot{q} = \frac{2\sqrt{\rho c k}}{\sqrt{\pi}} \sum_{i=1}^{m} \frac{T(0,t_i) - T(0,t_{i-1})}{\sqrt{t_m - t_i} - \sqrt{t_m - t_{i-1}}}, \tag{1}$$

with the thermal product $\sqrt{\rho c k}$ representing the properties density ρ, specific heat capacity c and thermal conductivity k of the thermocouple. The thermal product for each thermocouple is determined in the calibration process with a median value of 8600 $Ws^{0.5}/m^2K$ and an uncertainty of ± 300 $Ws^{0.5}/m^2K$. Considering this uncertainty in the material properties of the sensor, and in addition the uncertainties of all parts in the measuring chain, an uncertainty of less than $\pm$ 10 % in the final heat flux measurement is expected.

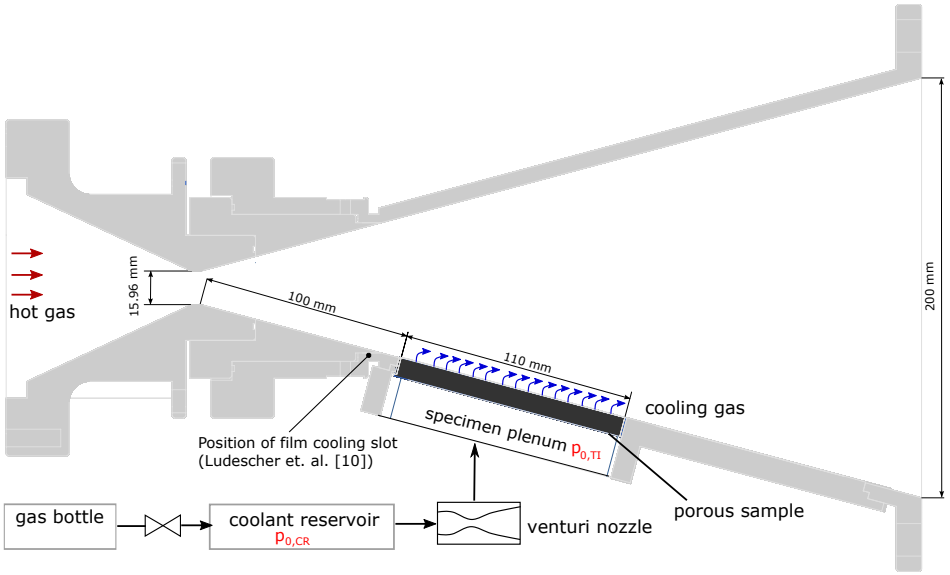

Fig 5. Location of the transpiration cooling experiment and flow scheme

The specimen is attached to conical nozzle which was initially installed for film cooling investigations, with the beginning of the porous segment placed 100 mm downstream of the nozzle throat as shown in Fig.5. The main geometric parameters of the nozzle are given in Table 2.

A schematic diagram describing the coolant flow scheme is shown right below the nozzle in Figure 5. The coolant mass flow is supplied by helium gas cylinders, feeding a coolant reservoir. The mass flow which is fed to the specimen plenum is controlled via a critical venturi nozzle. The massflow rate $\dot{m}_c$ trough a critical nozzle is given by

$$\dot{m}_c = p_{0,CR} A^* \sqrt{\frac{\gamma}{R T_{0,CR}} \left(\frac{2}{\gamma+1}\right)^{\frac{\gamma+1}{\gamma-1}}} \tag{2}$$

Table 2. Geometrical parameters of the conical nozzle

Parameter	Symbol	Unit	Value
Length of expansion part	L	mm	340
Throat Diameter	D_{th}	mm	15.96
Half opening angle	α	°	15
Curvature radius of throat	r_{curv}	mm	12
Expansion ratio	A_{exit}/A_{th}	-	157

For the measurements of this campaign, three different calibrated venturi nozzles (critcal diameters D^*_{vn} = 431 µm, 576 µm and 698 µm) have been used. Fig. 6 shows the pressure curve for the specimen plenum chamber of the transpiration inlet ($p_{0,TI}$) as well as the stagnation pressure upstream of the venturi nozzle ($p_{0,CR}$). The measured pressures were obtained using Kulite XCE-093-17 pressure sensors (accuracy $\pm$ 0.5% FSO). After the valve has opened, the pressure at the plenum chamber of the transpiration inlet increases due to the inflow of cooling gas. Steady conditions have been reached after 1 s. At this particular time, the outflowing mass of coolant into the main nozzle flow corresponds to $\dot{m}_c$.

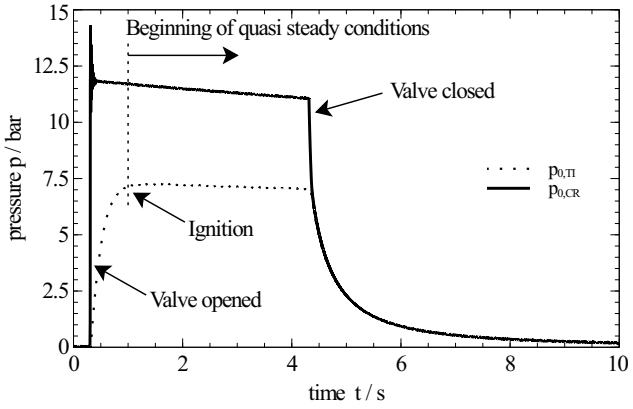

Fig 6. Pressure signals $p_{0,CR}$ and $p_{0,TI}$ for $\dot{m}_c$ = 0.27 g/s

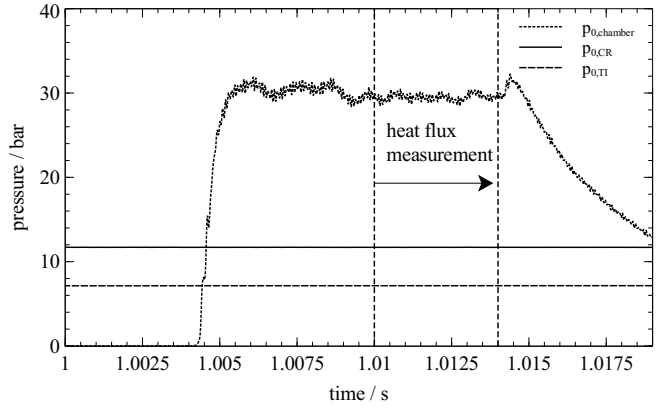

Fig 7. Pressure signals $p_{0,chamber}$, $p_{0,CR}$ and $p_{0,TI}$ for the experiment time

Fig.7 shows in detail the pressure levels during the experiment time frame relevant to the heat flux

measurement additionally displaying the stagnation pressure apparent in the nozzle stagnation chamber. After the pressures in the coolant reservoir and the specimen plenum have already reached their quasi-stationary conditions, the stagnation pressure rises sharply after the ignition of the hydrogen/oxygen mixture in the detonation tube and diaphragm burst up to the nominal stagnation pressure, reaching quasi-steady conditions at 1.01 s. The heat flux was measured between 1.01 s und 1.014 s.

3. Experimental Results and Comparison to Film Cooling

In order to investigate the effect of different mass flow rates on the cooling efficiency for both the porous wall and the wall affected by the wake flow, a parametric study with four different coolant mass flow rates was conducted. Furthermore, the measured cooling efficiencies are compared to theoretical cooling efficiencies for tangential film cooling.

3.1. Experimental Results

In the following, the results of the experimental study are described. To assess the magnitude of the heat flux reduction for the transpiration cooling experiments, a first reference measurement without cooling was performed with the porous specimen installed. The measured heat flux is shown in Fig. 8. Furthermore, simulation data of the setup from Ludescher and Olivier [10] are also shown. For these simulations, a turbulent chemical non-equilibrium flow was assumed, as this showed the best fit in parametric studies.

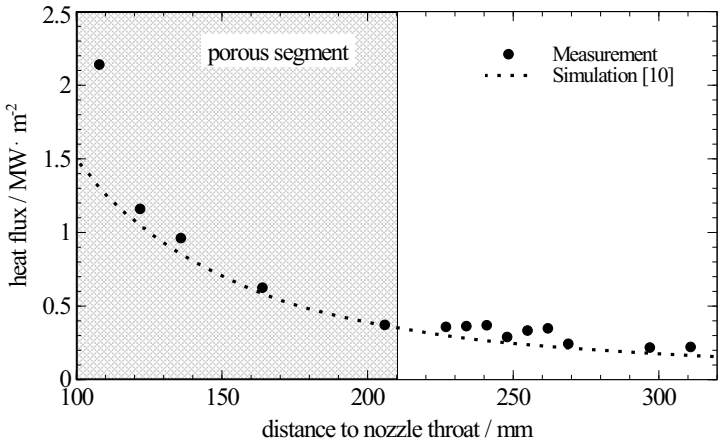

Fig 8. Measured and calculated heat fluxes without blowing

The measurement data shows the typical decrease of the heat flux over the nozzle length with further expansion of the hot gas flow, as shown in e.g. Ludescher [11], with a maximum heat flux of 2.1 MW/m^2. Repeat tests have determined a standard deviation of 4% from the average value. Furthermore, no signal could be retrieved from three thermocouples on the porous specimen

The simulation results, which assume chemical non-equilibrium and turbulent flow still show good agreement to the measurement data with the installed porous specimen, indicating that the implemented porous segment does not induce significant disturbances.

In the following, the results of the transpiration cooling experiments are being presented. The testing gas chosen for the transpiration cooling experiments is helium,which proved favorable for cooling applications [4, 10] due to its low molar mass and high specific heat capacity. The mass flow rate for both film and transpiration cooling can be expressed through the dimensionless blowing ratio

$$F = \frac{\dot{m}_c/A_c}{\dot{m}_{hg}/A_{hg}} = \frac{u_c \cdot \rho_c}{u_{hg} \cdot \rho_{hg}} \tag{3}$$

with the mass fluxes of the coolant and the hot gas. In this study, the mass flux density is taken from the

position at the nozzle throat with a value of $\dot{m}_{hg}/A_{hg}$ = 94.44 kg m^{-2}s^{-1}. In Table 5, the experimental parameters, as well as the resulting pressures inside the specimen plenum $p_{0,TI}$ are given.

Table 3. Test parameters for film cooling and transpiration cooling experiments

	Symbol	Unit	Case 1	Case 2	Case 3	Case 4
Mass flow rate Transpiration cooling	$\dot{m}_c$	g·s^{-1}	0.10	0.27	0.40	0.52
Blowing ratio Transpiration cooling	F	-	0.0013	0.0035	0.0052	0.0068
Venturi nozzle diameter	D_{vn}	µm	431	576	576	698
Specimen plenum pressure	$p_{0,TI}$	bar	3.9	6.2	7.8	9.7

To quantify the effectiveness of transpiration cooling, the cooling efficiency

$$\eta = 1 - \frac{\dot{q}_c}{\dot{q}_{nc}} \tag{4}$$

is introduced, with $\dot{q}_{nc}$ being the heat flux without cooling and $\dot{q}_c$ being the heat flux measured with cooling. The determined cooling efficiencies at the respective distances from the nozzle throat are being shown in Fig. 9. Over multiple retests a maximum standard deviation of 7% from the average value at a blowing ratio of F = 0.0068 has been determined.

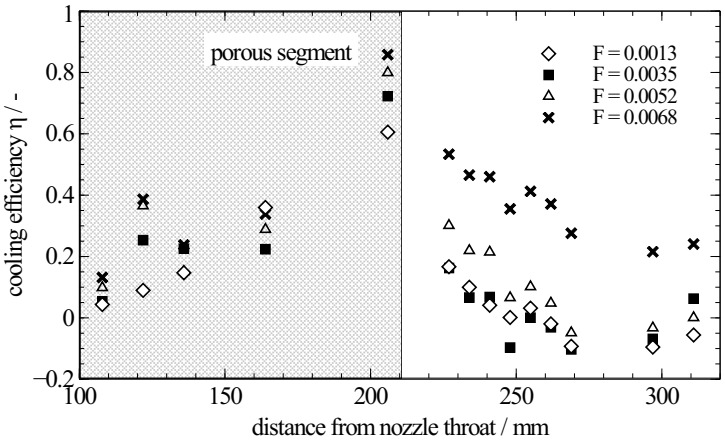

Fig 9. Cooling efficiency for different blowing ratios

For the investigated cases with transpiration cooling, two different phenomena were observed. First of all, over the porous sample the incoming heat flux steadily decreases, effectively raising the cooling efficiency at a blowing ratio of F = 0.0068 to 0.85 at the end of the porous segment. Moreover, as expected, increasing blowing ratio increases the cooling efficiency. Contrary to the general trend the second thermocouple showed significantly lower heat fluxes for F = 0.0035, 0.0052 and 0.0068 compared to the third and fourth thermocouple, leading to significantly higher cooling efficiencies. The cause for this deviation has not been found yet.

Secondly, in the wake flow, a significant influence of the different blowing ratios was observed, depending on the blowing ratio. Considering low blowing ratios with the case of F = 0.0013, the heat flux ratio reaches the same level as without blowing soon after the porous sample showing that no significant cooling effect created by a cooling film could be measured. However further downstream, the measured heat fluxes are even higher than without blowing, resulting in values of η < 0. These negative cooling efficiencies might be induced by enhanced turbulence levels induced by the cooling gas injection.

However, the measured heat fluxes in the wake flow of the porous sample are low, resulting in higher uncertainties in the determined cooling efficiencies. For high blowing ratios as for F = 0.0068, a much longer lasting cooling effect was observed. In this case, the wall heat flux up is being reduced up until the end of the instrumented section, with η = 0.21 at the last thermocouple position. This shows that with transpiration cooling relatively high blowing ratios are needed for achieving an effective and lasting cooling effect in the wake flow.

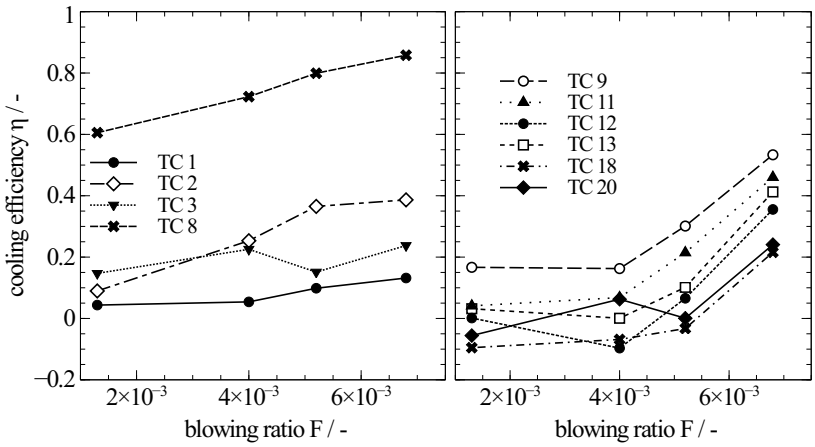

Fig 10. Influence of the mass flux on heat flux reduction over the porous sample (left) and in the wake flow (right)

Fig. 10 shows the dependency of the cooling efficiency on the blowing ratio. The cooling efficiencies are taken from four positions on the porous sample (TC1-3, TC8) and six positions in the wake flow (TC9-13, TC18, TC20). The increase of the cooling efficiency shows a correlation to the blowing ratio at each measurement position. At TC8 located at the end of the porous sample, the cooling efficiency increases from 0.6 at F = 0.0013 to 0.0085 at F = 0.0068. In the wake flow, the cooling efficiencies show an almost exponential increase with rising blowing ratios, e.g. at TC9 located directly after the porous sample, with comparably low cooling efficiencies at F = 0.0013 and F = 0.0040 which increases to 0.54 at F = 0.0068. This leads to the conclusion that for the investigated blowing ratios, transpiration cooling proves as being very effective even with low blowing ratios, creating an significant cooling effect over a porous nozzle segment with a low coolant mass flow demand. However, for creating an significant cooling effect in the wake of the porous segment a rather high blowing ratio is required.

As the presented study was intended as a preliminary study for the potential of transpiration cooling in a rocket engine nozzle, the results have to be interpreted cautiously due to limitations of the experimental setup. As the sample is comparably narrow, the measured heat flux values may be manipulated due to vortices forming at the interface between the porous section and the solid nozzle wall. Furthermore, due to the rectangular shape of the porous segment integrated into a conical nozzle the influence of the three-dimensional expansion in the nozzle could not be accounted for. These effects are expected to further intensify heat transfer at the position of the thermocouples, even higher cooling efficiencies are expected with an ideal transpiration cooling specimen. To quantify the influence of these three-dimensional effects, extensive studies using computational fluid dynamics simulations have to be performed.

3.2. Comparision to Film Cooling

To assess the potential of transpiration cooling, the experimental results described in Section 3.1 are compared to tangential film cooling as the state-of-the-art cooling method for nozzle extensions. Extensive fundamental investigations on film cooling were performed by Ludescher and Olivier [10], however, the experimental data are not directly comparable to this study, as the injection starts at different positions in the expansion nozzle as pointed out in Fig. 5. To obtain a comparable case, the theoretical film cooling efficiencies are calculated based on a approach described in [10], which was experimentally

validated for the given facility:

$$\eta_{Film} = \left[1 + \frac{7c_{p,hg}\delta(x)}{8c_{p,c}Fs}\frac{r(x)}{r_{curv}}\right]^{-1} \tag{5}$$

The boundary layer thickness $\delta(x)$ is calculated using a correlation assuming turbulent flow over a flat plate

$$\delta = 0.376xRe^{-0.2} \tag{6}$$

which is a valid approximation for slender nozzles. The starting point for x is the injection point.

As the aim of the study is a simplified comparison of film and transpiration cooling, the cooling methods are compared by analyzing the cooling effectiveness for both methods with a equivalent coolant mass flow rate. For determining a equivalent film cooling blowing ratio F_{Film}, it has to be taken into account,

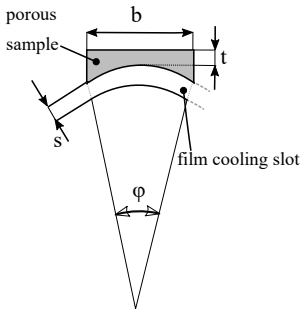

Fig 11. Description of lengths and angles for the experimental setup

that the transpiration cooling element spans only over a small angular range of the nozzle, while a film cooling slot would be circumferential. This will be expressed through the injection angle span ϕ, defined by the angle range between the cooled and uncooled nozzle segments in radial direction. For the film cooling case, ϕ_{film} is 360° due to the circumferential film cooling slot. For the transpiration cooling, the transpiration cooling element covers only 15.17° over the whole nozzle at the injection point as shown in Figure 11. It follows that the effective mass flow rate for the transpiration cooling experiments is given by

$$\dot{m}_{Transpiration} = \dot{m}_{Film}\left(\frac{\varphi_{Transpiration}}{\varphi_{Film}}\right). \tag{7}$$

The injection parameters for Equation 5 were chosen in accordance with the mentioned film cooling experiments using helium as test gas, the slot height s was assumed as 0.46 mm.

Table 4. Parameters at injection point

Condition	Symbol	Unit	Value
Specific heat capacity coolant	$c_{p,hg}$	J·(kg K)$^{-1}$	5193
Specific heat capacity hot gas	$c_{p,hg}$	J·(kg K)$^{-1}$	2897
Density hot gas	ρ_{hg}	kg·m^{-3}	0.0203
Mach number hot gas	M_{hg}	-	3.35
Velocity hot hot gas	u_{hg}	m·s^{-1}	3771
Slot height	s	mm	0.46

The respective parameters are given in Table 4. The hot gas parameters were calculated for the using the NASA CEA program [14], with a chemically frozen flow assumption after the nozzle throat [10, 15]. The resulting film cooling parameters are given in Table 5.

Table 5. Test parameters for film cooling and transpiration cooling experiments

	Symbol	Unit	Case 1	Case 2	Case 3	Case 4
Blowing ratio Transpiration cooling	$F_{Transpiration}$	-	0.0013	0.0035	0.0052	0.0068
Mass flow rate Transpiration cooling	$\dot{m}_{c,Transpiration}$	$g \cdot s^{-1}$	0.10	0.27	0.40	0.52
Mass flow rate per angle span	$\dot{m}'_c$	$g \cdot (s\ °)^{-1}$	0.0063	0.017	0.026	0.034
Mass flow rate Film Cooling	$\dot{m}_{c,Film}$	$g\ s^{-1}$	2.26	6.32	9.49	12.4
Blowing ratio film cooling	F_{Film}	-	0.31	0.85	1.28	1.67

The results for the theoretical film cooling efficiency and the transpiration cooling efficiency for the respective comparable mass fluxes according to Table 5 are shown in Fig. 12.

For the film cooling, the cooling efficiency is highest directly after the coolant slot and then steadily decreasing. For the transpiration cooling, the cooling effect increases steadily over the porous sample due to the slow film accumulation, reaching values of up to 0.85 for $F_{Transpiration}$ = 0.0068 at the end of the porous sample. Afterwards, a sharp decrease of the cooling efficiency could be observed due to the quick weakening of the coolant film, similar to low blowing tangential film cooling.

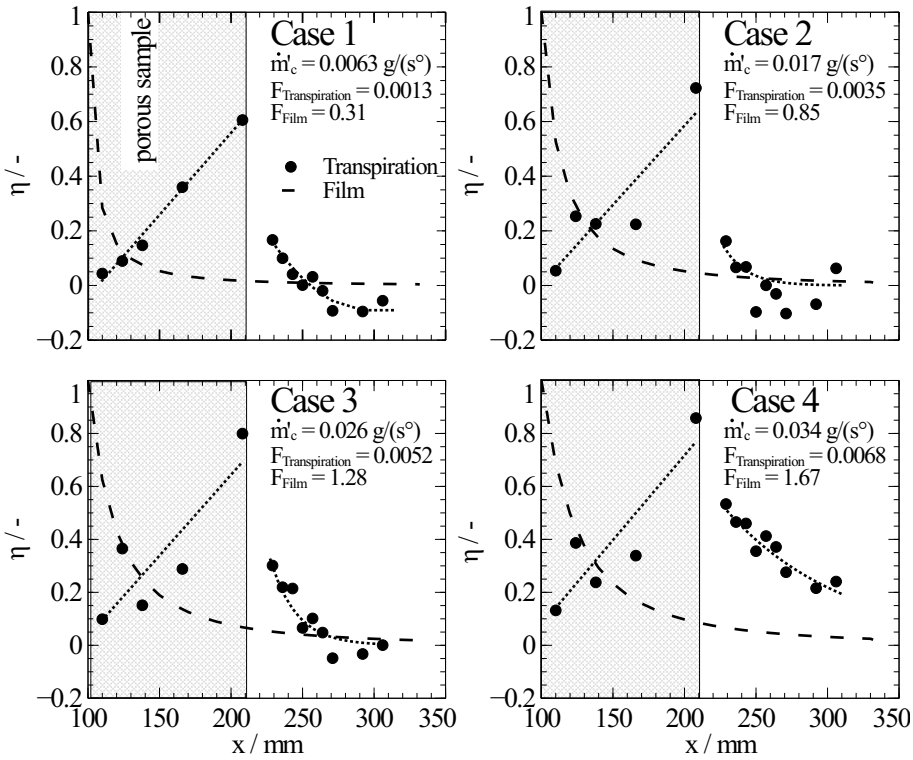

Fig 12. Comparision between film and transpiration cooling

When directly comparing the cooling efficiency of tangential film cooling to the cooling film created by orthogonal blowing, it can be generally seen that a ”break-even”-point exists, at which tangential film cooling and transpiration cooling have the same cooling efficiency. Downstream of this point, transpiration cooling is more efficient than transpiration cooling. For this point, a strong dependency on the coolant mass flow rate could be observed. With increasing coolant mass flow rate, the ”break-even” point moves further away from the injection point. This shows that transpiration cooling is highly effective over the porous segment even for very low blowing ratios. However, for a lasting cooling

effect even in the wake of the porous section, comparably high blowing blowing ratios are required. Here, Case 4 is an interesting example, as the film cooling efficiency decreases to almost 0 at the end of the investigated segment. However, for the transpiration cooling, a significant cooling efficiency of η = 0.24 could be determined for this measurement position, demonstrating a long lasting cooling effect by combined transpiration cooling and a lasting film cooling effect in the wake of the porous sample.

In conclusion, in the direct vicinity to the injection point, film cooling has a far better cooling performance, which can not be matched by transpiration cooling due to the effective cooling film created by the tangential cooling slot with a high coolant fluid momentum. Further downstream, transpiration cooling shows the positive effects of creating a cooling effect which is constantly renewed by distributing the same amount of coolant over a larger porous segment. However, high coolant mass flow rates are required for creating a significant cooling effect even at larger distances to the end of the porous outflow area.

As already mentioned in section 3.1, the experimental data may be influenced by three-dimensional flow phenomena due to the narrow specimen, which covers only a small portion of the nozzle circumference. This makes a direct quantitative comparison between the film and transpiration cooling experiments difficult. However, qualitatively, the preliminary experiments are showing promising results, as high cooling efficiencies and long-lasting cooling effects could be determined for the given setup. As even lower wall heat fluxes would be expected for an ideal transpiration cooling setup which would omit such phenomena, this underlines the potential of transpiration cooling as a highly efficient cooling method for rocket engine nozzles.

Despite its promising cooling effectiveness over the porous sample, it has to be kept in mind, that transpiration cooling imposes constraints on the nozzle design for rocket engine applications. Here, a coolant reservoir is needed on the backside of the cooled porous wall, making transpiration cooling only suitable for actively cooled structures. Due to its better performance in creating an effective and long-lasting cooling film, tangential film cooling is suitable to further decrease thermal loads on otherwise only radiatively cooled structures e.g. ceramic-matrix composite nozzle extensions. Furthermore, a combination of both film and transpiration cooling is being considered as a viable option for nozzle cooling. By superimposing a tangential cooling film with transpiration cooling, the tangential film cooling might compensate for the low cooling effectiveness at the beginning of a transpiration cooled nozzle segment.

4. Conclusion and Outlook

A preliminary study on transpiration cooling under supersonic rocket engine nozzle-like conditions were performed. The experiments were performed at a shock tube facility, creating a hot gas flow with stagnation temperatures of T_0 = 3660 K and stagnation pressures of p_0 = 30 bar. A porous ceramic matrix composite specimen inserted in the divergent part of a convergent-divergent conical nozzle was supplied with different coolant mass flow rates of helium. In order to determine the effect of different blowing ratios on the cooling efficiency, the heat flux on the nozzle wall was measured on the the porous specimen and in the wake flow of the porous segment. It could be shown, that a significant reduction of the heat flux on the porous segment could be achieved for all blowing ratios, with increasing cooling efficiencies for rising blowing ratios. A cooling efficiency up to 0.85 at the end of porous specimen with a blowing ratio of F = 0.0068 could be achieved. In the wake of the porous segment, the cooling effect quickly diminishes for low blowing ratios. To create a lasting cooling effect in the wake flow, rather high blowing ratios are required in order to create an effective cooling film.

The specific characteristics of transpiration cooling compared to tangential film cooling could be identified. While the efficiency of film cooling is very high in the direct vicinity of the injection slot and decreases steadily further downstream, transpiration cooling creates a cooling effect which increases with the length of the the porous sample. In the wake of the porous sample, the film cooling effect decreases significantly faster than for tangential blowing. A strong dependency of the cooling efficiency

on the film running length and the mass flow could be shown. Whereas tangential film cooling has a far better cooling efficiency near the injection point even at high transpiration blowing ratios, with longer running lengths transpiration cooling is advantageous due to the constant renewal of the cooling film, showing a far better performance than film cooling at the same specific mass flow rate.

However, the experimental data have to be interpreted with caution, as the influence of three-dimensional flow phenomena on the measurement values has to be investigated using CFD simulations. Here, based on the simulation results the porous nozzle section may have to be improved for future detailed studies which will focus on the development of analytical models describing the cooling efficiency in order to create design tools for rocket engine nozzle cooling applications.

Funding Sources

Financial support has been provided by the German Research Foundation (Deutsche Forschungsgemeinschaft - DFG) in the framework of the Collaborative Research Center Transregio 40: Technological Foundations for the Design of Thermally and Mechanically Highly Loaded Components of Future Space Transportation System.

References

[1] Winterfeldt, L. ; Laumert, B. ; Tano, R. ; James, P. ; Geneau, F ; Blasi, R. ; Hagemann, G.: Redesign of the Vulcain 2 Nozzle Extension. In: *2005 Joint Propulsion Conference* (2005)

[2] Shine, S.R. ; Nidhi, S. S.: Review on film cooling of liquid rocket engines. In: *Propulsion and Power Research* 7 (2018), March, Nr. 1, S. 1–18

[3] Eckert, E.R.G. ; Livingood, J.N.B.: Comparison of Effectiveness of Convection-, Transpiration-, and Film-cooling Methods with Air as Coolant / National Advisory Commitee for Aeronautics. 1953 (3010). – Technical Note

[4] Langener, T. ; Wolfersdorf, J. von ; Selzer, M. ; Hald, H.: Experimental investigations of transpiration cooling applied to C/C material. In: *International Journal of Thermal Sciences* 54 (2012), April, S. 70–81

[5] Stollery, J.F. ; El-Ehwahny, A.M.M.: A note on the use of a boundary-layer model for correlatng film-cooling data. In: *International Journal of Heat and Mass Transfer* 8 (1965), Nr. 1

[6] Librizzi, J. ; Cresci, R. J.: Transpiration Cooling of a Turbulent Boundary Layer in an Axisymmetric Nozzle. In: *AIAA Journal* 2 (1964), April, Nr. 4, S. 617–624

[7] Goldstein, R.J. ; Eckert, E.R.G. ; Wilson, D.J.: Film Cooling With Normal Injection Into a Supersonic Flow. In: *Journal of Manufacturing Science and Engineering* 90 (1968), November, Nr. 4, S. 584–588

[8] Chen, F. ; Bowman, W. J. ; Bowersox, R.: Effect of transpiration cooling on nozzle heat transfer. In: *Journal of Spacecraft and Rockets* 33 (1996), Nr. 3, S. 453–455

[9] Keener, D. ; Leenertz, J. ; Bowman, W. J. ; Bowersox, R.: Transpiration cooling effects on nozzle heat transfer and performance. In: *Journal of Spacecraft and Rockets* 32 (1995), Nr. 6, S. 981–985

[10] Ludescher, S. ; Olivier, H.: Experimental Investigations of Film Cooling in a Conical Nozzle Under Rocket-Engine-Like Flow Conditions. In: *AIAA Journal* 57 (2019), March, Nr. 3, S. 1172–1183

[11] Ludescher, S.: *Supersonic film cooling in generic rocket nozzles*. PhD Thesis, RWTH Aachen University, 2020

[12] Yahiaoui, G. ; Olivier, H.: Development of a short-duration rocket nozzle fow simulation facility. In: *AIAA Journal* 59 (2015), Nr. 9, S. 2713–2725

[13] Cook, W. J.: Determination of Heat-Transfer Rates from Transient Surface Temperature Measurements. In: *AIAA Journal* 8 (1970), July, Nr. 7, S. 453–455

[14] Gordon, S. ; Mcbride, B.J.: Computer program for calculation of complex chemical equilibrium compositions and applications / NASA Lewis Research Center. 1994 (1311). – NASA Reference Publication

[15] Sutton, G. P. ; Biblarz, O.: *Rocket Propulsion Elements*. Hoboken, New Jersey : John Wiley & Sons, 2010